JOM
https://doi.org/10.1007/s11837-019-03340-y




# Nanofibrils as Building Blocks of Silk Fibers: Critical Review of the Experimental Evidence

QIJUE WANG[1] and HANNES C. SCHNIEPP[1,2]

1.—Applied Science Department, William & Mary, Williamsburg, VA 23187 8795, USA. 2.—e-mail: schniepp@wm.edu

Silks have fascinated researchers for decades, featuring outstanding mechanical performance and vast potential as a multifunctional material. Development of synthetic fibers mimicking natural silk is a major goal but has been hindered by insufficient knowledge of the silk structure. Nanoscale fibrils have long been suggested to play a significant role in silk; in this review, we examine prior evidence of nanofibrils in spider and silkworm silks. We found the available data far from conclusive. The volumetric percentage of nanofibrils in silk fibers is totally unclear, and conflicting results have been reported regarding their physical dimensions, morphology, and spatial organization. Some works have proposed an entirely different, globular nanostructure of silk fibers. Hence, many of the structural models were developed based on incomplete evidence. Our review highlights the gaps in knowledge about the nanostructure of silk fibers and can act as a guide for future studies.

## INTRODUCTION

Silk has been an invaluable multipurpose material for millennia, with applications ranging from medical sutures over military equipment to clothing.[1,2] The outstanding combination of high strength and high extensibility of silk has fascinated materials scientists for decades,[3–6] hoping to achieve such desirable performance in mass-produced synthetic materials.[7–10] To this end, sufficient knowledge of the structure–property relationships of silk is needed,[3] which is not met by our current level of understanding. Synthetic silk fibers currently do not match the performance of natural silks,[7,9–11] and neither the hierarchical structure of these natural materials nor their synthetic counterparts are understood in detail.

Nanofibrils have been suggested to play a role as structural building blocks and have been subject to experimental investigation[12–20] as well as to modeling.[19,21–24] Evidence suggesting the presence of these protein fibrils has been found in various kinds of silk fibers, however, with reported diameters spanning a significant range of 3–300 nm.[25,26] Interestingly, nanofibrillar structures have been shown to be the major component in other structural biomaterials optimized for tensile loadings,[27] such as collagen,[28] cartilage,[29] tendon,[30] and synthetic cellulose-based materials.[19,31,32] Several researchers have proposed that nanofibrils contribute significantly to the mechanical performance of silk and have carried out corresponding theoretical analyses.[12–14,16,21] The concept of nanofibrils as a structural component of silks has inspired many researchers to develop schematic models describing the hierarchical structure of silk, prominently featuring nanofibrils.[13,19,21,23,33–38] However, as we will show in more detail, the available experimental evidence for nanofibrils is still limited, and an unambiguous characterization of even the basic properties of nanofibrils has yet to be established. No consensus regarding the diameters, lengths, or concentration of nanofibrils in silk fibers has been reached, and only a small number of silk producing species has been investigated. Given this degree of uncertainty, it might seem surprising that dozens of works in the literature have further propagated the idea of nanofibrils as important building blocks of silk fibers, seemingly insensitive to the ambiguity and uncertainty we have found in a rigorous analysis of the available evidence.

Here we review all available evidence regarding nanofibrillar features in silk fibers from spiders and silkworms. We first discuss the most common sample preparation and characterization techniques; then, we review the evidence on spider

Published online: 23 January 2019

and silkworm silk. An extensive discussion pointing out the critical issues in this field and potential solutions is provided. We further examine the proposed structural models of natural silks and review the degree to which they are in agreement with available experimental results as far as nanofibrils are concerned.

## EXPERIMENTAL METHOD

As a protein-based material, natural silk is prone to alterations caused by physical and chemical sample preparation techniques,[12,14,33,39,40] which we discuss first. Then, we look into the different characterization techniques used to reveal the structure of silk regarding their advantages, disadvantages, and special implications for silk studies.

### Sample Preparation

The most commonly studied spider silk is the major ampullate (MA) silk from orb-weaving spiders, usually featuring a cylindrical shape with a diameter of several micrometers.[14,41–43] Once the functional coating is removed, observation of the fiber surface is straightforward using microscopy. To expose the internal structure of the silk fiber for further analysis, chemical or physical methods have to be used. Chemical methods to remove the outermost parts of the fiber and reveal its interior used solutions of $Na_2CO_3$,[23,44] LiBr,[14,45] urea,[14,42] hydrochloric acid,[14] and hexafluoroisopropanol (HFIP).[12,14,39] Physical means to expose the fiber's inside involved scratching,[12] stretching,[12,14,15,33,43] peeling,[18,44] ultramicrotomy,[14,22,25,41,43,46] and polishing.[47] Although these methods provide access to the internal material of silk fibers, they all bear the risk of altering or damaging the natural fiber structure. The results of subsequent characterizations thus have to be assessed carefully as to what extent they represent the altered rather than the native structure of silk (Fig. 1).

### Electron Microscopy

One of the most widely used techniques to image the structure of silk is electron microscopy (EM),[12,13,26,39,40,43,44,47,48] featuring high spatial resolutions. For scanning electron microscopy (SEM), a resolution of several nanometers can be conveniently achieved at a very high depth of field, thus, delivering realistic high-resolution images.[49] For transmission electron microscopy (TEM), the resolution is even better than 1 nm.[50] Another important consideration is that EM offers the ability to easily and quickly zoom from millimeter to nanometer length scales without any sample or equipment modification. Furthermore, recent work by Wan et al.[51] showed the potential to distinguish crystalline and amorphous regions in silk fibers using secondary electron hyperspectral imaging. These advantages make SEM and TEM powerful tools to investigate the nanoscale structures of silk fibers.

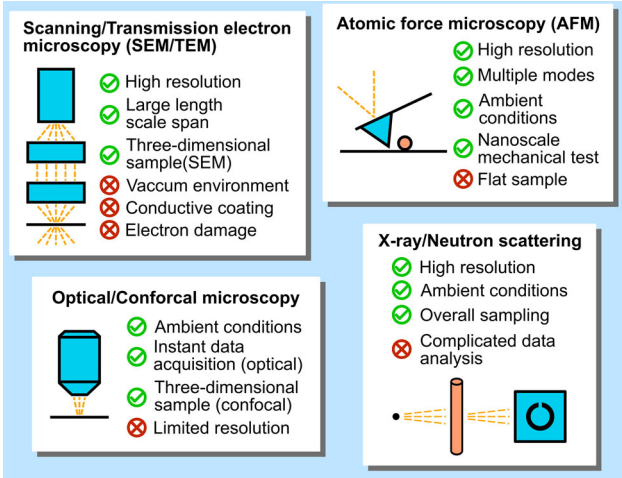


Fig. 1. Comparison of the advantages and disadvantages of the different experimental techniques used to study silk fibers.

However, these attractive functionalities come with several requirements and limitations. First, a high vacuum environment is necessary to obtain good electron beam performance. Consequently, volatile components, most importantly water, are removed from the fiber in this process. Removal of water may significantly alter the fiber structure, especially regarding the secondary structure of the silk protein.[1,45] Second, a conductive coating is usually applied before SEM imaging to avoid charging of the sample and subsequent image distortions. Conductive coatings come with the risk of covering or blurring the smallest sample features that are sometimes most interesting. On high-end SEM equipment, the charging can be managed without a conductive coating, which avoids these problems altogether.[51] Finally, silk fibers easily suffer from the damage caused by the electron beam during the imaging procedure, thus, introducing another risk of altering the delicate protein nanostructures of interest.

### Atomic Force Microscopy

Another powerful tool employed to investigate the structure in silk fibers is atomic force microscope (AFM).[12,13,17,18,22,25,33,39,40,43,44,46,52] Like the SEM, AFM can provide resolutions on the order of a few nanometers. In addition to the sample's surface topography, AFM can reveal valuable information like surface friction and stiffness.[17,53] Furthermore, with the ability to perform force spectroscopy and other mechanical tests.[5,54] AFM provides unique capabilities.

One major limitation of AFM is the requirement of a flat sample surface. In particular, scanning a cylindrical silk fiber with its typical diameter of

several micrometers simply placed on a flat substrate poses a nontrivial challenge for AFM imaging. Consequently, additional sample preparation steps were typically employed to obtain good AFM images.[17] Ultramicrotomes, in which sharp blades of diamond or glass remove layers of the sample, were used in several studies to slice silk fibers.[14,22,25,41,43,46] This method reduces the topography for AFM imaging and exposes the internal fiber structure. However, this procedure can be considered aggressive as it introduces a significant amount of shear and normal stresses and thus comes with a significant risk of altering the natural internal structure of the silk fiber. Moreover, any unevenness of the cutting knife can introduce linear surface textures that can easily be mistaken for fibrillar structures.

### Optical Microscopy

Optical wide-field and confocal microscopies have also been used to investigate silk fibers.[14,41,42] Their advantage is that silk fibers can readily be investigated nondestructively and without some of the limitations that other imaging techniques bring with respect to sample flatness or electrical conductivity. Complicated sample preparation is not required, and imaging can be carried out relatively easily under ambient conditions.

The most severe limitation of optical far-field techniques is the spatial resolution given by the diffraction limit $\Delta x$. Best realistic resolutions in the visible spectrum are obtained using blue light with a wavelength of $\lambda$ = 400 nm and an oil immersion objective featuring a numerical aperture of up to N.A. = 1.4. The resulting diffraction limited resolution is $\Delta x = \lambda/(2\ \text{N.A.}) \approx 140$ nm. Furthermore, experiments using short wavelengths bear the risk of altering the mechanical behaviors of natural silk fibers.[55] Another downside of optical techniques is the limited depth of field, which becomes especially severe for microscope objectives with high magnification and high N.A. This significantly limits the microscope's ability to image three-dimensional samples, which can be alleviated by confocal microscopy, albeit at a significantly higher cost for equipment and increased data acquisition and processing time.

### Scattering Techniques

Scattering techniques like wide-angle and small-angle x-ray scattering (WAXS/SAXS), neutron scattering, and electron scattering offer alternative routes to investigate nanofibrillar structures in silk.[16,18,56,57] Scattering techniques provide an "inverse space" representation of the sample, including its smallest features. The signal obtained via scattering is usually an equal representation of the entire sample exposed to the beam. This situation is complementary to imaging techniques operating in "real space" and provides both limitations and opportunities. Imaging techniques have the advantage of directly producing a highly magnified representation of the sample. However, with increasing spatial resolutions, smaller and smaller regions of the sample are assessed, which comes with a risk of selecting an area that is not representative. Scattering, on the other hand, does represent the entire sample, or at least the region sampled by the beam. However, it is not clear which features or parts of a sample give rise to a particular feature in the scattering signal. An interesting study transcending these traditional limitations has recently been carried out by Riekel et al.[16] using x-ray nanodiffraction. In this work, the x-ray beam with a diameter of several hundred nanometers was scanned across a silk sample, thus, providing a series of diffractograms, each representing a small region of the sample. Hence, this approach combines advantages from both imaging and scattering techniques.

A principal limitation of scattering techniques is that the three-dimensional structure of the sample is translated into a two-dimensional or even a one-dimensional intensity pattern by the diffraction process, in which the phase information is lost. Consequently, a complete reconstruction of the sample structure from the diffraction pattern is not possible. Given a hypothesis about the sample structure, the diffraction pattern can be calculated from the hypothetical structure and compared to the measured pattern. Discrepancies can be addressed by iterative modifications to the model. This process can be time consuming, without a guarantee for obtaining the correct structure; because of the information loss in the scattering process, many different structures give rise to the same diffraction pattern. Additionally, like all high-energy beams, x-rays may alter or damage the sample. This complicates structural analysis because it is not clear whether the observed structure is native or due to radiation exposure.

## NANOFIBRILS IN NATURAL SPIDER SILK

### *Nephila* Genus

Many works have examined silk fibers. At this point, however, less than 20 different kinds of spider and silkworm silk fibers have been studied in detail.[20] Given that there are over 46,000 species of spiders alone,[58] each one making its own kinds of silk, this is a tiny fraction of the silks found in nature. A silk type studied particularly often is the MA silk of the *Nephila* (*N.*) genus. One of the first works discussing nanofibrils from this genus was published in 1994 by Li et al., who investigated microtomed internal surfaces of *N. clavipes* MA silk and concluded that the observed patterns represented a pleated fibrillar structure with diameters ranging from 100 nm to 300 nm (Fig. 2a).[25] However, the AFM images provided in this study were not of high enough resolution to identify fibrils

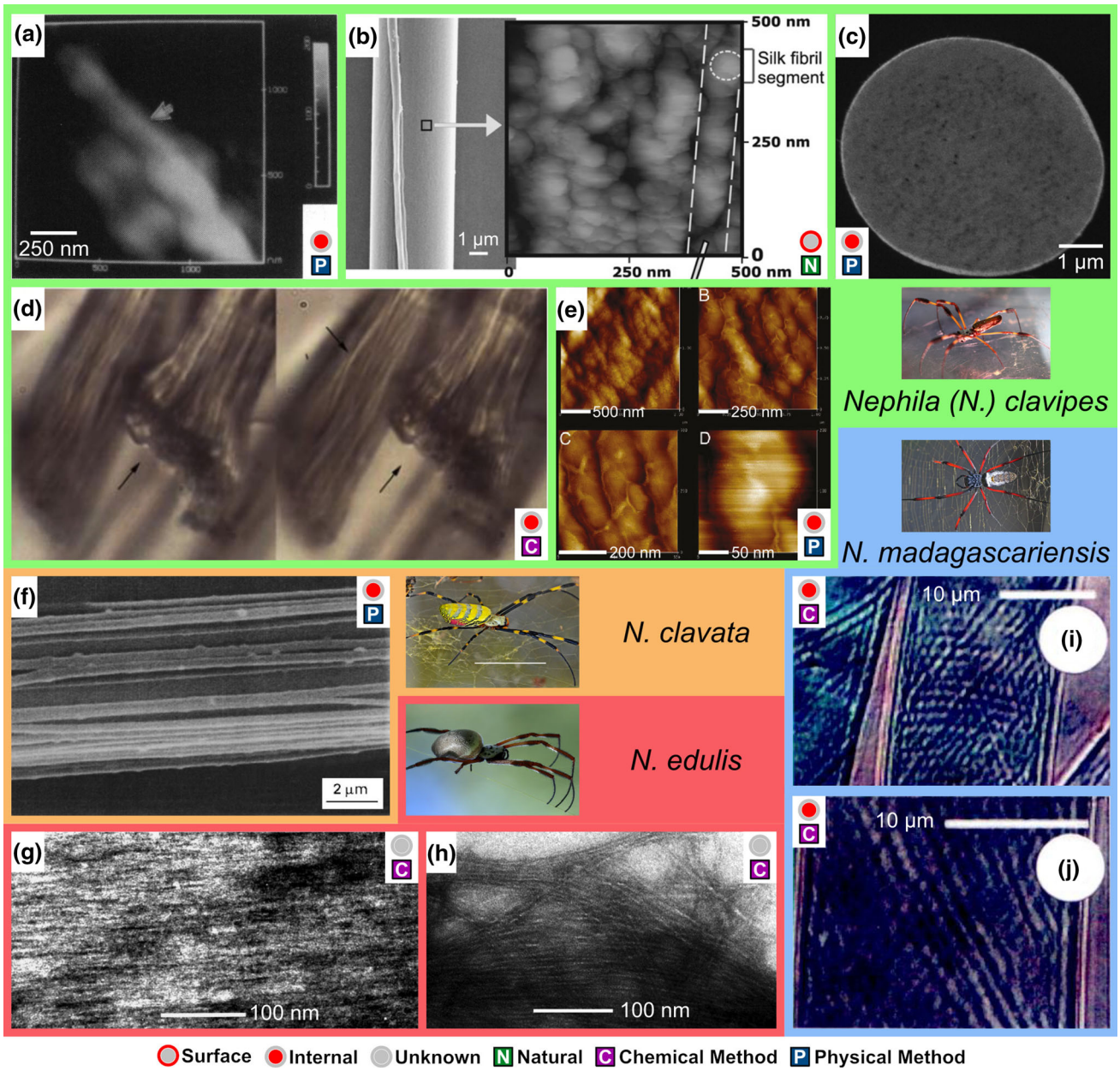


Fig. 2. Experimental evidence of nanofibrils in major ampullate (MA) silk from the *Nephila (N.)* genus. Colors of the panel frames indicate the species—green: *N. clavipes*; orange: *N. clavata*; red: *N. edulis*; blue: *N. madagascariensis*. (a) Atomic force microscopy (AFM) topography of the pleated fibrillar structure inside the fiber.[25] Vertical range: 0–200 nm. (b) Fiber surface showing 40–80 nm large segments.[13] Left: Scanning electron microscopy (SEM) image of a dragline silk. Right: AFM topography of the silk surface. No vertical range was provided. (c) Confocal microscopy image of *Nephila* silk cross section showing the skin–core organization.[41] (d) Stereo micrograph of fibrillar structure in *Nephila* silk.[14] No size information was provided. (e) AFM topography images of 200-nm-wide nanofibrils on the ultramicrotomed silk surface.[22] No vertical range was provided. (f) SEM image of the abraded surface of *N. clavata* silk showing many nanofibrils.[15] (g, h) Transmission electron microscopy (TEM) images of nanofibrils of ≈ 3 nm in width observed in chemically dispersed *N. edulis* silk.[26] (i, j) Optical microscope images of the "criss-crossing" fibrillar pattern observed in *N. madagascariensis* silk.[42] Permissions: (a) Adapted from Ref. 25. Copyright 1994 Biophysical Society. (b) Adapted from Ref. 13. Copyright 2006 Biophysical Society. (c) Adapted from Ref. 41. Copyright 2006 John Wiley and Sons. (d) Adapted from Ref. 14. Copyright 2007 Sponner et al. (e) Adapted from Ref. 22. Copyright 2012 American Chemical Society. *N. clavata* image reprinted from Ref. 59. Copyright 2015 Hoebeke et al. (f) Adapted from Ref. 15. Copyright 1997 Chapman and Hall. (g, h) Adapted from Ref. 26. Copyright 2002 Royal Society. *N. edulis* image provided by Graham Winterflood for one-time use. (i, j) Adapted from Ref. 42. Copyright 1996 Royal Society. *N. madagascariensis* image provided by Jerry Oldenettel for one-time use (Color figure online).

unambiguously. In 1997, Yang et al.[56] investigated the same MA silk with SAXS and concluded that there were fibrils with a diameter as small as 6 nm. For the following two decades, various techniques were employed to study the nanofibrillar structure of MA silk fibers from *N. clavipes*,[14,18,22,41] *N. pilipes*,[13] *N. edulis*,[26,57] *N. clavata*,[15] as well as *N. madagascariensis*.[42] Segmented nanofibrils were

reported to be on the fiber surface, with segments sized 40–80 nm (Fig. 2b).[13] However, for both slow- and fast-reeled fibers, these segments appeared to be more disconnected rather than closely connected and thus could not obviously be assigned to contiguously formed nanofibrils.[13] Most of the literature investigating *Nephila* MA silk focused on the interior of the fiber. By studying the microtomed[14,41] or fractured[43] cross section of the MA silk via AFM, SEM, and TEM, a skin–core organization and functional coatings on top of the skin layer were identified. Using confocal microscopy, the diameter of observed fibrils was determined to be 100–150 nm (Fig. 2c),[41] which is surprising given that the lower end of this range is below the diffraction limit of far-field optics. Another study found the fibrils to be parallel to the fiber axis but twisted, which was suggested to prevent cracks from propagating (Fig. 2d).[14] More recently, nanofibrils that are 200 nm in diameter were identified via AFM and found to have 100 nm wide, and 150-nm-long globular protrusions distributed along their axes (Fig. 2e).[22] This is in agreement with the previously reported, segmented structure on the fiber surface (Fig. 2b),[13] although the physical sizes of the segments are different. Currently, the most clear evidence supporting a fibrillar structure within the bulk of *Nephila* (*N. clavata*) MA silk is provided by the SEM images obtained by Kitagawa et al.[15] The abraded surface of *N. clavata* silk fiber showed fibrils with diameters around 100 nm (Fig. 2f). Unfortunately, the sample preparation conditions of this study could not be reproduced since.

Two studies of *Nephila* silk are noteworthy. Using TEM, Knight et al.[26] found nanofibrils as thin as 3 nm in *N. edulis* dragline silk (Fig. 2g and h) after the fiber was dispersed with a Silversen homogenizer at 4°C and negatively stained in aqueous 2% ammonium molybdate. Unfortunately, no additional details regarding the sample preparation for this interesting study were provided. Vollrath et al.[42] used optical microscopy to investigate stained fibers that were soaked and swollen in urea. They observed fibrils (Fig. 2i and j) that were aligned but at various angels with respect to the fiber axis, forming a "criss-crossing" lattice. A similar organization was reported for black widow spider silk fibers,[52] and for several silkworm silks[44] (see details below).

A review of all the evidence for *Nephila* silk shows an ambiguous situation, where the variations in the reported nanofibril morphology are significant. The structures observed via AFM (Fig. 2b and e) tend to be more segmented rather than obviously fibrillar, while other techniques emphasize the fibrillar character more strongly. The reported fibril dimensions cover a large range spanning two orders of magnitude, from 3 nm to ≈ 300 nm. Finally, we caution that the circular shapes and spherical protrusions observed (Fig. 2c) in the cross section of *Nephila* silk are not necessarily a proof for the existence of nanofibrils but could also be globules or granules distributed within the silk fiber. Interestingly, no fibril pullout—a natural result of fibrillar organization—was observed in this case. As a matter of fact, globular structures have been found in other types of spider silk (see below). To provide a more direct conformation for the existence of nanofibrils, longitudinal cross sections running parallel to the fiber axis would be helpful (previous works[14,25] provided limited clues), rather than cross sections oriented perpendicular with respect to the fiber axis.

## Other Spider Species

The structure of the MA silk of several other spider species was examined, including the black widow (*Latrodectus hesperus*), where AFM topography images revealed the existence of nanofibrils with diameters of 60 ± 30 nm on the fiber surface[52] (images of strained fibers shown in Fig. 3a and b). Interestingly, the nanofibrils were not aligned with the fiber axis but at an angle of 69° ± 3°. AFM was also used to investigate the surfaces of *Nephilengys cruentata* (MA) (Fig. 3c and d) and *Avicularia juruensis* (acinous gland) silk (Fig. 3e and f) strands using lateral force (Fig. 3c and e) and amplitude images (Fig. 3d and f).[17] Only the lateral force data of *Nephilengys cruentata* silk (Fig. 3c) hinted at a fibrillar structure; while the authors did not provide the dimensions of these nanofibrils, our assessment of Fig. 3c suggests an average nanofibril diameter of ≈ 17 nm.

Riekel et al.[16] used nano-SAXS technique to examine the MA silk of *Argiope bruennichi*. They concluded that the skin layer is composed of nanofibrils with diameters of 100 nm, while the nanofibrils in the core region were suggested to have a diameter of 6.3 nm. Interestingly, an investigation of the related species *Argiope trifasciata* MA silk revealed globular structures rather than nanofibrils.[43,46] SEM was used to image fracture surfaces of *Argiope trifasciata* MA silk, where small, round features with diameters of ≈ 100 nm were observed (Fig. 3g and h).[43] The authors interpreted these round features as faces of nanofibrils. As previously discussed, mere observation of round features is not a proof for the existence of nanofibrils; other morphologies, such as globules, would give rise to similar features in the cross-sectional view. A later study[46] investigated silk fibers that were ultramicrotomed longitudinally, i.e., featuring a cross section parallel to the fiber axis (see insets to Fig. 3i and j). The authors studied both supercontracted (Fig. 3i) and forcibly silked (Fig. 3j) fibers. Interestingly, no evidence of nanofibrils was found (Fig. 3i and j); instead, globular surface features were reported, which are incompatible with nanofibrils running parallel to the fiber axis. The diameters of the observed globules were 10 ± 2 nm and 13 ± 4 nm in supercontracted and forcibly silked strands, respectively.

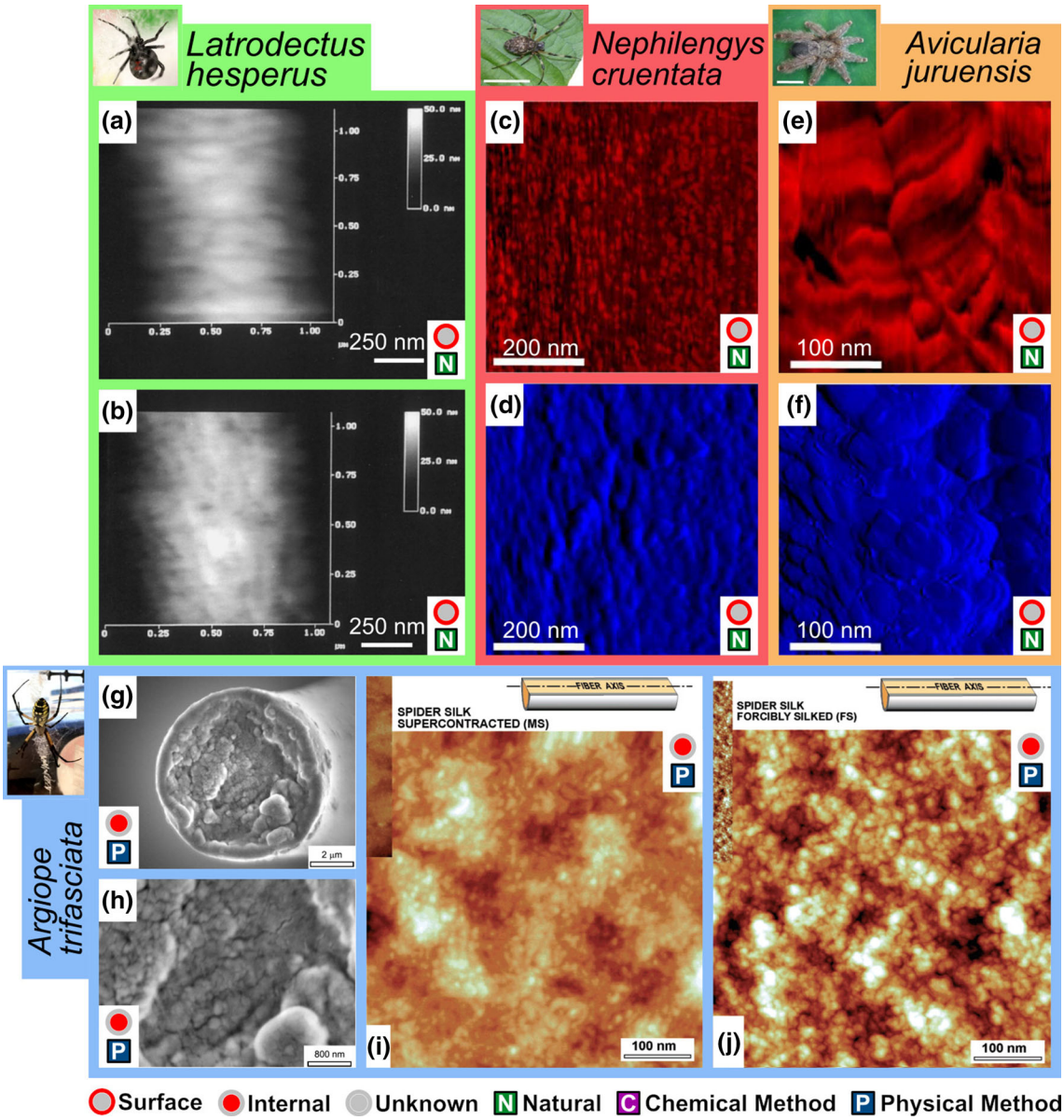


Fig. 3. Observation of nanofibrils/globules in the MA silks from several spider species. Colors of the panel frames indicate the species. Green: *Latrodectus hesperus*; red: *Nephilengys cruentata*; orange: *Avicularia juruensis*; blue: *Argiope trifasciata*. (a, b) AFM topography images of fibrillar structures found on the surface of strained fibers.[52] Vertical ranges: (a, b) 0–50 nm. (c, e) AFM lateral force images of surface features on fiber surface.[17] (d, f) AFM amplitude images of surface features on fiber surface.[17] (g, h) Globular structures found on the fracture surface of a fiber.[43] (i, j) Globular features found on the longitudinal surfaces of supercontracted and forcibly silked MA silk fibers.[46] Permissions: (a, b) Adapted from Ref. 52. Copyright 1999 Elsevier Science B. V. (c–f) Spider images of *Nephilengys cruentata* and *Avicularia juruensis:* adapted from Ref. 17. Copyright 2013 Springer Nature. (g, h) Adapted from Ref. 43. Copyright 2002 Elsevier Science Ltd. (i, j) Adapted from Ref. 46. Copyright 2007 American Chemical Society.

The MA silk from the recluse (*Loxosceles*) spider is particularly interesting: unlike the cylindrical MA silk spun by most spiders, *Loxosceles* silk features a thin ribbon morphology with 6–8 $\mu$m in width and around 50 nm in thickness.[5,6,12,60] Although this morphology is in stark contrast to virtually all other silks, it provides unique opportunities to further the understanding of the structure–property relationships of silk. It is currently the only silk for which the size, length, and volume fraction of nanofibrils have been completely determined.[12] Since the silk virtually entirely consists of 20 nm (width) × 7 nm (thickness) nanofibrils (Fig. 4), it also provides an opportunity to directly assess the nanofibrils' mechanical properties based on macroscopically measured fiber tensile properties.[12] Importantly, the mechanical behavior of the fiber is similar to MA dragline silks in terms of modulus, strength, extensibility, and toughness.[5,6,12] This suggests the possibility that the molecular-scale and nanofibril-scale properties of this silk are similar to other silks, thus, providing an interesting window to understanding silks.

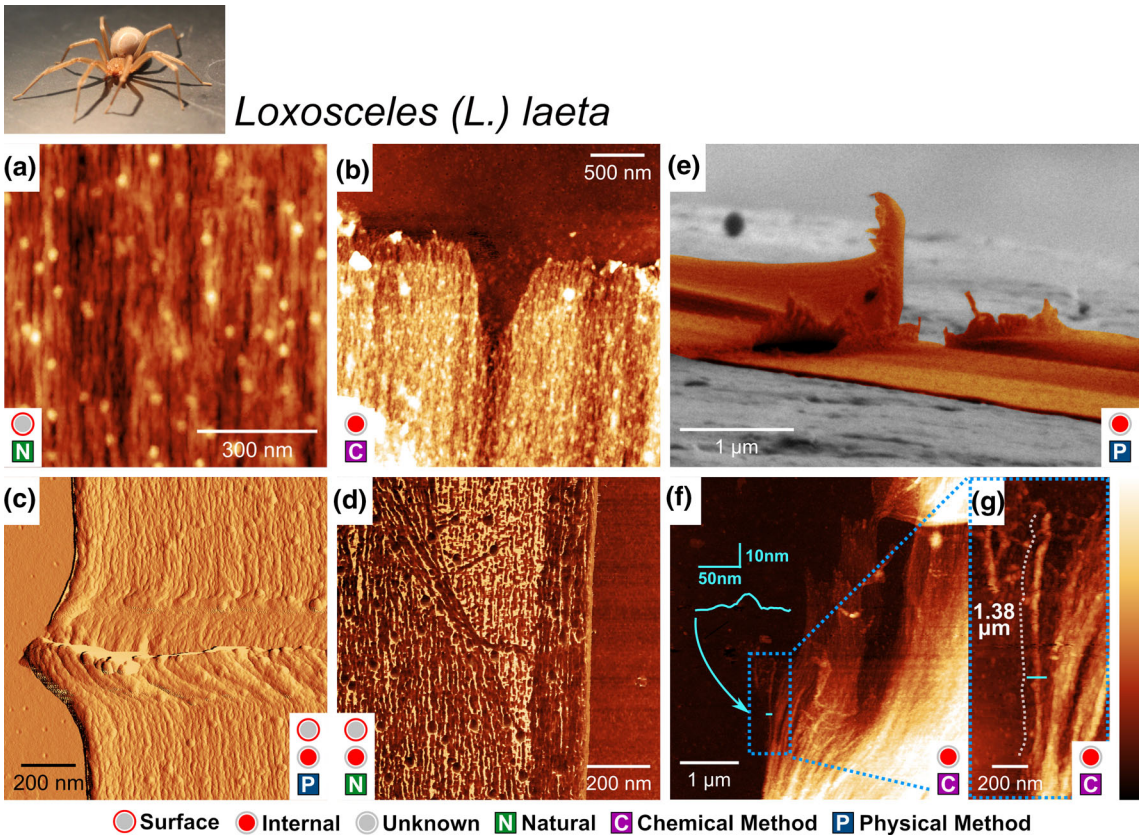


Fig. 4. Observation of nanofibrils in *Loxosceles (L.) laeta* silk.[12] (a) AFM topography of nanofibrils with 20 nm diameter on the silk ribbon's surface. (b) A single nanofibril layer observed in the partially dissolved ribbon (AFM topography), with an average thickness of 7 nm, determined by several cross sections (yellow curves). (c) AFM magnitude image of a trench made by AFM scratching, within which nanofibrils can be seen. (d) AFM phase image of a surface defect exposing the nanofibrils underneath. (e) In situ SEM image (false colored) of a single *Loxosceles* ribbon right after being cut by a focused ion beam (FIB), showing numerous nanofibrils pointing away from the fracture surface. (f, g) AFM topography of a single nanofibril in the partially dissolved ribbon. This fibril was measured to be 1.38 $\mu$m long. Color bar: (a) 0–18 nm; (b) 0–17 nm; (f) 0–60 nm; (g) 0–30 nm. Permission: panels (b), (d), (e)–(g) are adapted from Ref. 12. Copyright 2018 American Chemical Society.

Since spider silk proteins (spidroins) have a relatively large molecular weight, around 250–350 kDa,[1,53,61,62] the 50-nm-thick silk ribbon of the recluse spider can only accommodate a limited number of these molecules.[62] On the silk surface, nanofibrils can be identified directly (Fig. 4a). To investigate the internal structure of *Loxosceles* silk, several methods were employed: (1) When the ribbon silk was partially dissolved by HFIP, a single layer of nanofibrils was obtained (Fig. 4b). (2) With AFM-based scratching, a trench with a depth of half the ribbon thickness was made perpendicular to the silk axis (Fig. 4c), in which nanofibrils were found. (3) A surface defect shown in Fig. 4d features an opening of the topmost layer of nanofibrils, revealing the fibrils beneath. (4) Silk ribbons cut with a focused ion beam (FIB) showed numerous nanofibrils pointing in different directions (Fig. 4e). No other structural constituents were found; the nanofibrils are the sole structural element in *Loxosceles* silk. Furthermore, much information was gained about how these nanofibrils arrange into the whole silk ribbon: they are loosely bonded (Fig. 4d and e) and organized in a "pseudo-layered" structure (Fig. 4b–d). Most importantly, individual nanofibrils were isolated from partially dissolved silk ribbons (Fig. 4f and g). This allowed us to determine that all nanofibril lengths were $> 1$ $\mu$m.[12]

Although the great majority of studies on spider silk have focused on MA silk, famous for its high strength and toughness, it is important to note that a female orb-weaver spider can produce up to seven different kinds of silk, each specialized for a different task.[1,35] These other types of silk have mostly been studied to determine their protein structures;[58,63–69] only little is known about their structural makeup. Hakimi et al.[47] found parallel nanofibrils in the egg sac silk (cylindriform silk) of *N. edulis*. Globular structures were found in the minor ampullate silk of *Argiope trifasciata*.[70] It is worth noting there are also the cribellate silks, which are an entirely different kind of silk featuring a three-dimensional network of fibrils featuring diameters of only several tens of nanometers.[71]

## NANOFIBRILS IN NATURAL SILKWORM SILK

### *Bombyx (B.) mori* and Other Silkworm Silks

The silk produced by silkworm *Bombyx (B.) mori* (image above Fig. 5a) has been more widely investigated (Fig. 5) than the silk from any other species.[18,23,39,43,44,48,72] For our discussion here, it will be treated side-by-side with the silk from the Atlas moth (*Attacus atlas*),[43] the Chinese tussar moth (*Antheraea (A.) pernyi*),[44,47] and the Japanese oak silk moth (*Antheraea yamamai*),[33,44] all featured in Fig. 6.

After removing the sericin coating from the fibers (degumming), the surface can readily be observed, which revealed 20- to 30-nm nanofibrils (Fig. 5a–c).[23,48,72] These linear features have segmented subunits, similar to what has been reported for the surface of *Nephila* silk (Fig. 2b),[13] although the segments are smaller in *B. mori* silk.

As for the internal structure, the most extensive and detailed studies were carried out by Putthanarat et al.,[44] Poza et al.,[43] Hakimi et al.,[47] and Pérez-Rigueiro et al.[46] The silk fibers produced by *B. mori* (Fig. 5d–f), *A. pernyi* (Fig. 6a), and *A. yamamai* (Fig. 6c) were degummed and then peeled,[43,44] microtomed (Fig. 5g–i for *B. mori*), or fixed in resin and then polished (Fig. 5j for *B. mori*, Fig. 6b for *A. pernyi*)[47] to expose their internal structure. Unlike the skin–core organization found in cylindrical spider silks,[14,41,43] the *B. mori* silk features two irregularly shaped central protein brins.[23,43,47] Based on AFM and SEM observations (Fig. 5d–j),[23,43,46,47] the protein brins contain numerous nanofibrils parallel to the fiber direction, which were found to be 60–200 nm in diameter.[18,43,44,46] Layers of nanofibrils were found on peeled surfaces of *B. mori*, *A. pernyi*, and *A. yamamai* silk fibers.[44] The layered makeup is similar with the "pseudo-layered" structure found in the *Loxosceles* spider silk.[12] However, the layers found in the *Loxosceles* silk are flat and strictly parallel (Fig. 4c and d), while the layers in these silkworm silks are aligned at various angles. These angled layers resemble the lattice network found in *Nephila*[42] (Fig. 2i and j) and *Latrodectus* (Fig. 3a) MA silks.[52]

In a more drastic approach of chemical sample treatment,[39] HFIP was used to completely "exfoliate" the *B. mori* fibers and harvest the nanofibrils produced in this process (Fig. 5k). These nanofibrils were found to be 20 nm in diameter and 300 to 500 nm in length.[39] Similarly, the more recent work by Niu et al. used a mixture of NaOH/urea to completely exfoliate *B. mori* fibers,[40] which yielded 30 nm diameter fibrils (Fig. 5l). From these fibrils, they further isolated silk nanoribbons, featuring a width of 25 nm and a thickness of 0.4 nm (Fig. 5m).

Several interesting results were obtained from silk fibers produced by worms other than *B. mori*. Zhang et al. recently showed that *A. yamamai* silk has better mechanical properties than *B. mori* silk,[33] which was attributed to a different fracture mode. The fracture surface of *A. yamamai* silk showed numerous fibrils sticking out from the fiber (Fig. 6d and e); *B. mori* silk, in contrast, showed a flat fracture surface, without any visible fibrils, which was interpreted as a brittle fracture mode.[33,43] The authors suggested that the fibrillar organization in case of *A. yamamai* prevented crack propagation, thus, avoiding brittle fracture.[33] For *Attacus atlas* silk, much larger fibrils, termed "microfibers," rather than nanofibrils were observed (Fig. 6f and its inset).[43]

## DISCUSSION OF THE AVAILABLE EVIDENCE

For an overview of the reported evidence regarding nanofibrils in silk and to facilitate a systematic discussion, we summarized all the data in Table I. It is organized by species, with information regarding the employed characterization techniques, the dimensions of observed fibrillary structures, the location examined within the fiber, and any applied sample treatments.

### Most Critical Unresolved Issues

It would be desirable to develop a consensus model for the structure of silk fibers. One challenge is that many different species produce silk fibers, and at this point, it is not yet clear to what degree a single model will be applicable across many species. Our review shows that the available information is still scarce, scattered across different species, characterizations, and sample preparation techniques, so that there are significant gaps in our understanding. Further experiments will be needed to close these gaps and resolve some of these issues. The most severe unresolved discrepancies and open questions are discussed first.

One fundamental issue is that not all studies have concluded that the nanostructure within a silk fiber

Fig. 5. Evidence for nanofibrils in *Bombyx (B.) mori* silk. Image above (a): *B. mori* silkworm. (a–c) Nanofibrils observed on the degummed fiber surface.[23,48,72] Scale bars: (a) 100 nm, (b) 75 nm. (d) AFM topography of the fibrillar structure on the peeled surface.[18] (e, f) SEM images of fibrillar structure on the peeled surface.[44] (g–i) AFM topography of nanofibrils on the microtomed fiber surface.[43,46] (j) SEM image of the polished fiber fixed in resin, showing linear nanofibrils.[47] (k) SEM image of liquid-exfoliated nanofibrils deposited on the substrate.[39] (l) SEM image of the NaOH/urea-dissolved silk fiber featuring ≈ 30-nm-diameter nanofibrils.[40] (m) AFM topography of exfoliated silk nanoribbons (width: 25 nm, thickness: 0.4 nm).[40] Permissions: (a) Adapted from Ref. 72. Copyright 2013 Royal Society of Chemistry. (b) Adapted from Ref. 23. Copyright 2010 John Wiley and Sons. (c) Adapted from Ref. 48. Copyright 1998 American Chemical Society. (d) Adapted from Ref. 18. Copyright Elsevier Science B. V. (e, f) Adapted from Ref. 44. Copyright Elsevier Science Ltd. (g, h) Adapted from Ref. 43. Copyright Elsevier Science Ltd. (i) Adapted from Ref. 46. Copyright 2007 American Chemical Society. (j) Adapted from Ref. 47. Copyright 2006 American Chemical Society. (k) Adapted from Ref. 39. Copyright 2016 John Wiley and Sons. (l, m) Adapted from Ref. 40. Copyright 2018 American Chemical Society.

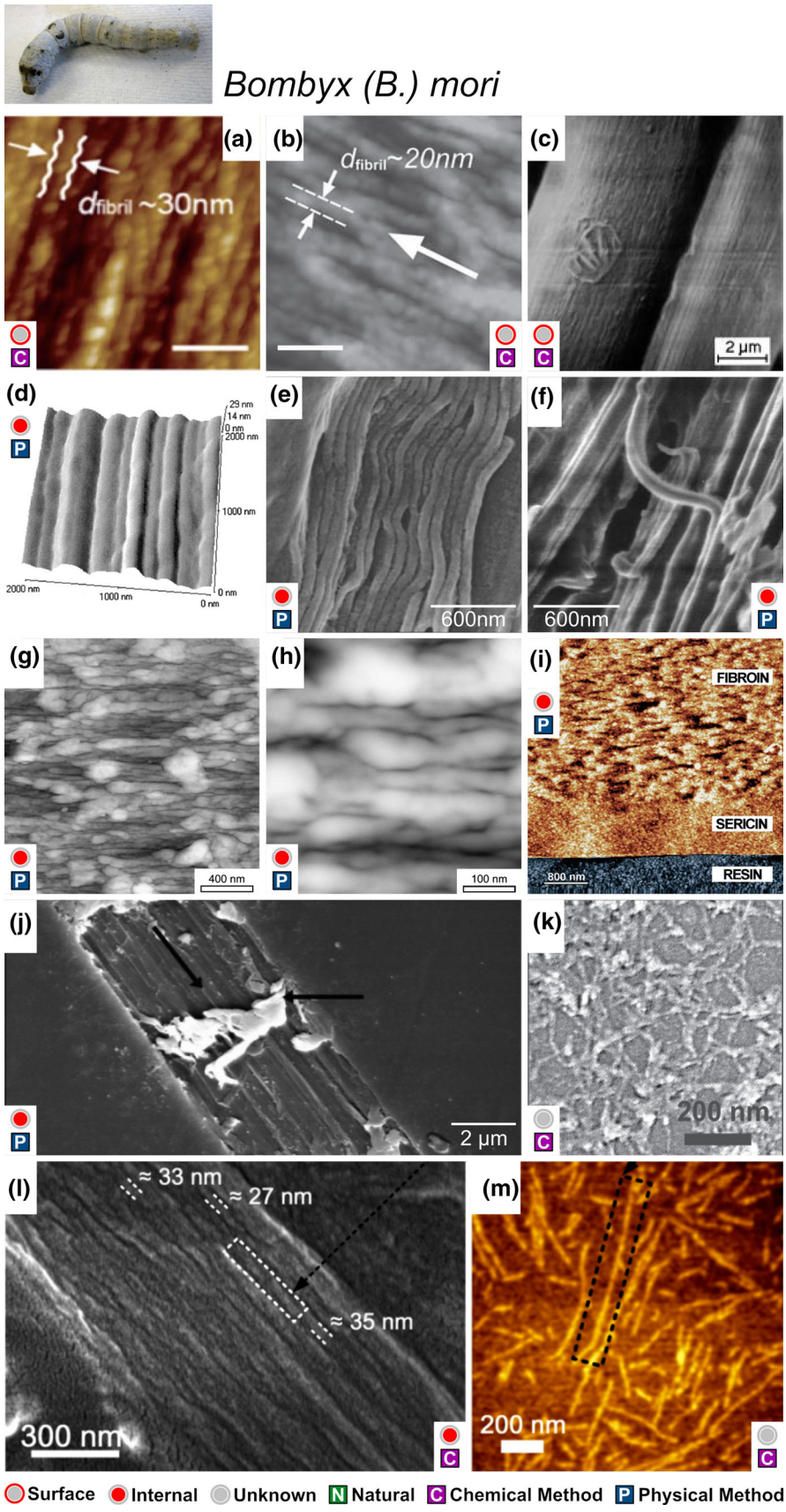
Bombyx (B.) mori
(a)
$d_{fibril}$ ~30nm
(b)
$d_{fibril}$~20nm
(c)
2 µm
(d)
29 nm
14 nm
0 nm
2000 nm
1000 nm
0 nm
2000 nm
1000 nm
0 nm
(e)
600nm
(f)
600nm
(g)
400 nm
(h)
100 nm
(i)
FIBROIN
SERICIN
800 nm
RESIN
(j)
2 µm
(k)
200 nm
(l)
≈ 33 nm
≈ 27 nm
≈ 35 nm
300 nm
(m)
200 nm
Surface
Internal
Unknown
N Natural
C Chemical Method
P Physical Method

actually features a nanofibrillar morphology. Two AFM-based studies on *Argiope trifasciata* silk[43,46] instead reported globular structures with different dimensions. Globule diameters of 100 nm were found on the fracture surface (Fig. 3g and h),[43] whereas much smaller globules (less than 20 nm in diameter) were found on the microtomed surface of a supercontracted and forcibly silked fiber (Fig. 3i and j).[46] In contrast, a nano-SAXS study of the silk from *Argiope bruennichi*, a closely related species of the same genus, found a nanofibrillar morphology, in agreement with the majority of previous literature reports for cylindrical spider silks.[16] Since the contradicting studies employed different sample preparation techniques and different characterization methods, a detailed analysis may show that some of these methods are better suited for revealing the true structure than others. Microtoming the samples may well have an impact on the nanoscale organization of the protein and thus be a potential culprit for the observed morphological differences.

Another critical and perhaps surprising aspect of the available studies discussing silk nanostructures is that virtually all are completely silent when it comes to the volumetric fraction of nanofibrils in silk fibers. There is not even a coarse estimate as to whether nanofibrils make up a small fraction of a silk fiber or its majority. The only exception is *Loxosceles* silk, which is virtually entirely composed of nanofibrils (Fig. 4).[12] Without tangible information regarding the nanofibril concentration in silk fibers, it is difficult to develop an evidence-based model silk.

## Nanofibril Diameters

Estimates on nanofibril diameters have been made in many studies of silk fibers, and thus, a comparison of the obtained numbers provides a good overview regarding commonalities and discrepancies in the published data (Table I). Generally, the reported nanofibril diameters range from a few

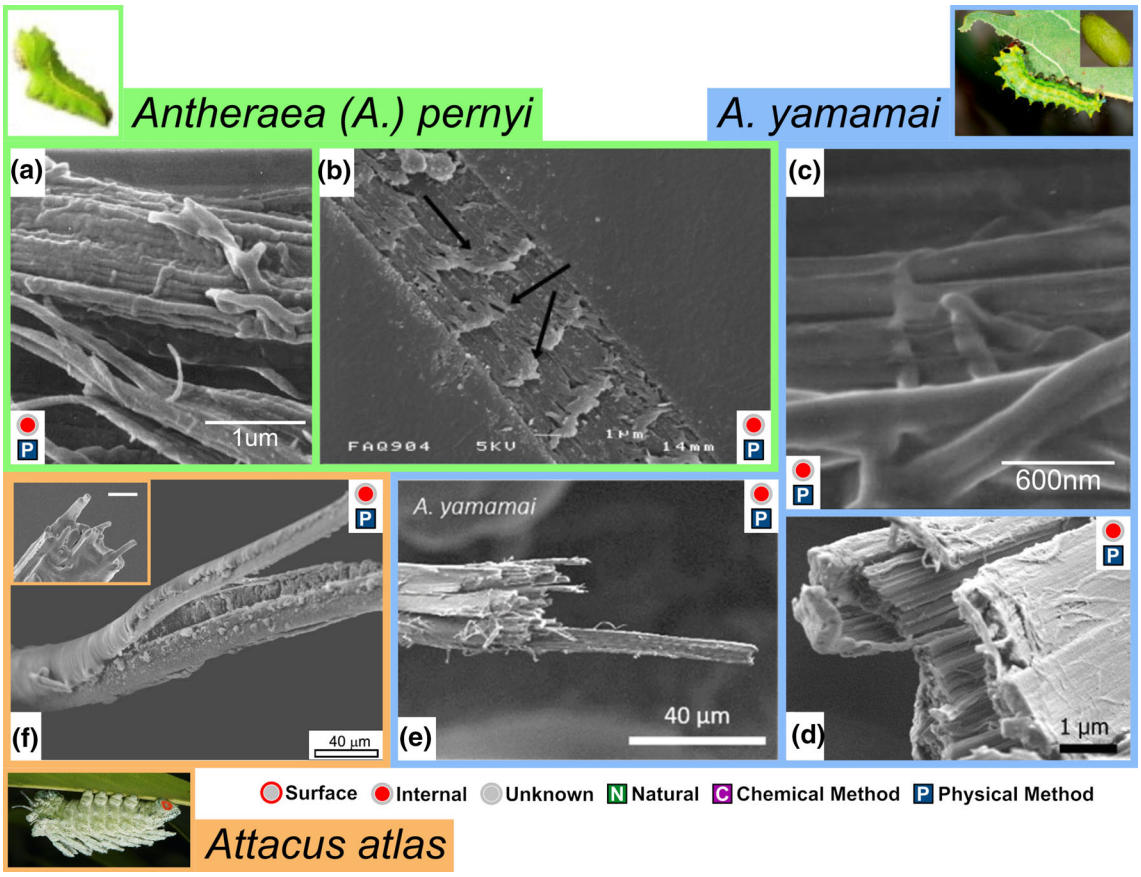


Fig. 6. Evidence of nanofibrils in the silks of several silkworm species. Panel frames in different colors indicate the species. Green: *Antheraea (A.) pernyi*; blue: *A. yamamai*; orange: *Attacus atlas*. (a, c) Surface of peeled fibers featuring fibrillar structures.[44] (b) SEM image of the polished fiber fixed in resin, showing linear nanofibrils.[47] (d, e) SEM images of fractured silk fibers, showing numerous nanofibrils.[33] (f) Fractured region of an *Attacus atlas* silk fiber.[43] Microfibrils with diameters of 1 $\mu$m rather than nanofibrils were identified. Inset scale bar: 7 $\mu$m. Permissions: (a, c) Adapted from Ref. 44. Copyright Elsevier Science Ltd. Image of *A. pernyi*: Reprinted from Ref. 73. Copyright 2015 Korean Society of Applied Entomology, Taiwan Entomological Society and Malaysian Plant Protection Society. (b) Adapted from Ref. 47. Copyright 2006 American Chemical Society. (d, e) and image of *A. yamamai*: Adapted from Ref. 33. Copyright 2018 American Chemical Society. (f) Its inset: Adapted from Ref. 43. Copyright Elsevier Science Ltd. *Attacus atlas* image provided by John Horstman/itchydogimages. All rights reserved (Color figure online).

**Table I. Summary of observed evidence of nanofibrils in different types of natural spider and silkworm silks**

| | Species | Methods | Width [nm] | Length [nm] | Location | Sample Treatment | Ref. |
|---|---|---|---|---|---|---|---|
| Spiders | *Nephila (N.) clavipes* | SAXS | 6 | 100 | Global | Natural | [56] |
| | | | 160 | 230 | | | [18] |
| | | AFM | 113±21 | 98±13 | Internal | Peeled surface | |
| | | OM | 100–150 (implied) | — | | Microtomed, freeze fractured, 8M urea | [14] |
| | | Confocal | 100–150 | — | | Semithin section slides | [41] |
| | | AFM | 100–300 | — | | Cryomicrotomed slides | [25] |
| | | | 200 | — | | Microtomed slides | [22] |
| | *N. pilipes* | SEM, AFM | 40–80 | — | Surface | Natural | [13] |
| | *N. clavata* | SEM | 100 | — | Internal | Abraded and ion-etched draglines | [15] |
| | *N. edulis* | WANS/ SANS | — | >170 | Global | Natural | [57] |
| | | TEM | 3 | — | Unknown | Dispersed at 4 °C | [26] |
| | *N. madagascariensis* | OM | — | — | Internal | 8M urea | [42] |
| | *Latrodectus hesperus* | AFM | 60 ± 30 | — | Surface | Natural | [52] |
| | *Argiope bruennichi* | Nano-SAXS | 100 | 100 | Skin | | [16] |
| | | | 6.3 | | Core | | |
| | *Argiope trifasciata* | SEM | Globules ≈100 | | Internal | Fractured | [43] |
| | | AFM | Globules: 10±2 (supercontracted) 13±4 (forcibly silked) | | | Stained, resin fixed, ultramicrotomed | [46] |
| | *Loxosceles laeta* | AFM, SEM | 20 | >1000 | Surface, internal | Natural, AFM cut, FIB cut, HFIP dissolved | [12] |
| | *Nephilengys cruentata* | AFM | ≈20[a] | — | Surface | Natural | [17] |
| | *Avicularia juruensis* | | — | — | | | |
| Silkworms | *Bombyx (B.) mori* | SAXS | 219 | 170 | Global | Degummed, peeled | [18] |
| | | AFM | 168±21 | 119±16 | Internal | | |
| | | | 100 | 1000–2000 | | Fractured, resin fixed, microtomed | [43] |
| | | | 90±30 | 600±200 | | Resin fixed, microtomed | [46] |
| | | AFM, SEM, TEM | 30 (fibril) 25 (ribbon) | — | Internal, dissolved | NaOH and Urea dissolved | [40] |
| | | AFM | 20 | — | Surface | Degummed | [23] |
| | | | 30 | — | | | [72] |
| | | SEM, TEM | 20 ± 5 | 300–500 | Unknown | HFIP dissolved | [39] |
| | | SEM | — | — | Surface | Degummed | [48] |
| | *B. mori, Antheraea (A.) pernyi* | SEM | — | — | Internal | Resin fixed, polished | [47] |
| | *B. mori, A. pernyi, A. yamamai* | AFM, SEM | 90–170 | — | | Degummed, peeled | [44] |
| | *A. yamamai* | AFM | 5 | — | Unknown | Dissolved | [33] |
| | | SEM | — | — | Internal | Fractured | |
| | *Attacus atlas* | | 1000 | — | | | [43] |

[a]Estimated by the authors of this paper from the published data.

nanometers to hundreds of nanometers; however, the studies were carried out with silks from different species, different locations within the fiber were targeted, samples were prepared in different ways, and different characterization techniques were employed.

In some cases, several studies were carried out on fibers from the same species, such as *B. mori*, which makes it easier to determine the sources of observed discrepancies and, ultimately, to develop a consensus model. For instance, a SAXS study reported a fibril diameter of 219 nm,[18] whereas studies using AFM, TEM, and SEM reported nanofibril diameters of 20–30 nm on samples made from dissolved fibers.[39,40] All these experiments are expected to sample the entire fiber equally rather than just investigating a particular region of the fiber. Hence, the observed discrepancy of about one order of magnitude may reflect differences of the employed sample preparation techniques. It is theoretically possible that the chemical dissolution techniques have an effect on the nanofibril diameter, for instance, by partially dissolving the nanofibrils themselves rather than simply separating them. This effect would indeed systematically underestimate the nanofibril diameter.

Another reason for the discrepancy in observed nanofibril diameters, and in this case perhaps the more likely one, may be the fact that different characterization techniques were employed (SAXS versus imaging techniques). Scattering techniques, such as SAXS, are generally capable of providing information about nanostructures at smallest length scales and thus have been widely used to study natural silks.[13,16,18,56,57,74–79] Surprisingly, however, only a few of these works provided hints about the nanofibrillar structure within the fibers.[16,18,56,57] This may suggest that scattering techniques are not particularly sensitive with respect to the detection of nanofibrils. This may explain why several x-ray scattering studies have yielded results that are difficult to bring into agreement with results from other techniques, or even with independently repeated x-ray experiments. For instance, SAXS studies of fibers of the same species, *N. clavipes*, have independently obtained contradictory nanofibril diameters of 6 nm and 160 nm.[18,56] Miller et al.[18] have proposed to improve the accuracy of x-ray data by adopting a two phase model[18] to calculate correlation lengths in the equatorial and meridional directions from SAXS scattering data. Through this method, they were able to get consistent nanofibril dimensions from both SAXS and AFM results. However, determining the origin of the observed discrepancies in reciprocal-space data remains challenging; in contrast, imaging techniques have the advantage that they visualize the structure of the sample, which may provide an additional check as to whether sample preparation was successful.

Another general observation is that fibril diameters reported on the fiber surfaces were in most cases $< 100$ nm,[13,17,23,52,72] usually 20–30 nm.[17,23,72] Interestingly, for a 5-$\mu$m-diameter silk fiber, a surface layer of 20-nm-thick nanofibrils would only make up 1.6% and is thus not necessarily representative of the bulk of the fiber. Fibrils imaged in the interior of fibers were systematically larger than fibrils observed on the surface, typically $> 100$ nm. On the one hand, this may reflect an actual difference in diameter based on the location. On the other hand, however, it may also represent differences in sample preparation since visualization of internal fibrils requires more invasive preparation techniques than surface imaging, often applying chemical treatments or significant mechanical forces to the sample, such as microtoming or fracturing.[14,22,25,41,43,46,47] These treatments may alter the protein structure and thus the observed nanofibril diameters. The latter idea is further supported by the fact that internal fibril diameters estimated on dissolved or exfoliated fibers, where no such mechanical treatments are required, did not show this increase in diameter compared to fibril diameters observed for surface fibers.[39,40] We thus hypothesize that the actual nanofibril diameter may indeed be as little as 20–30 nm for many species.

As noted above, several x-ray studies have suggested fibril diameters drastically different from other experimental techniques. Fibril diameters as small as 6 nm[56] and 6.3 nm[16] were found by SAXS. Interestingly, the latter work used nano-SAXS to also selectively study fibrils from the skin region of the fiber and concluded that they are much thicker, about 100 nm. However, this is exactly the opposite of the trend we saw in most of the other results: generally, fibrils observed on the surface were thinner than nanofibrils on the inside. Only two other studies, like the SAXS studied mentioned, had found fibril diameters substantially smaller than 20 nm: A TEM study of exfoliated *N. edulis* fibers showed 3 nm fibrils,[26] and an AFM study of dissolved *A. yamamai* fibers showed 5 nm fibrils.[33]

Based on the significant degree of uncertainty, spread of the data, sparse coverage across different species, and even direct contradiction between published results, the evidence regarding fibril diameters is still limited in terms of serving as a basis for a consensus model. In several cases, the size assessments were based on only a few images, or even a single image. Therefore, some of the published conclusions may have been drawn from nonrepresentative data.

## Length of Nanofibrils

An important aspect that has not been widely discussed is the length of nanofibrils. Since nanofibril length will have a substantial impact on the silk fiber's mechanical properties,[12] an accurate description of fibril length is necessary for a rigorous understanding of silk. Scattering experiments have provided some hints, with several studies suggesting nanofibril lengths in the range 100–230 nm.[16,18,56,57] Based on the difficulty of bringing x-ray data into agreement with other studies, there may be some limitations regarding the accuracy of

these findings. Imaging techniques would be critically important to validate some of these findings. However, only a few works measured the nanofibril length using imaging techniques, to the best of our knowledge. For *B. mori* silk, Poza et al.[43] reported 1- to 2-$\mu$m-long nanofibrils (AFM topography); Miller et al.[18] reported 119 ± 16 nm (AFM topography); Pérez-Rigueiro et al.[46] reported 600 ± 200 nm (AFM topography); and Ling et al.[39] reported 300–500 nm (SEM). For *N. clavipes* silk Miller et al.[18] reported 98 ± 13-nm-long nanofibrils via AFM topography images.

More recently, our group isolated individual nanofibrils from partially dissolved *Loxosceles* silk and found they were > 1 $\mu$m long.[12] However, we suspect that the actual length of the nanofibrils is much greater, since the applied chemicals may have broken up the fibrils.

Several factors may contribute to the lack of evidence on nanofibril length: (1) Isolating individual nanofibrils from natural silk fibers has proven to be challenging.[12] (2) When the nanofibrils are still a part of the entire fiber formation, as typically imaged, it is difficult to identify the beginning and end points of individual nanofibrils. (3) Imaging conditions that will capture the entire length of a nanofibril, yet provide resolutions at the single nanofibril level—which is necessary to determine the end points of a fibril—are difficult to achieve.

## Organization of Nanofibrils Within the Fiber

An interesting angle that did not get significant attention is the question of whether or how the nanofibrils are organized within the fiber. This discussion may seem premature, since not even the concentration of nanofibrils within the fiber has been established. However, several studies have suggested that silk fibers from spiders (*Nephila,*[42] *Latrodectus*[52]) and from the silkworm (*B. mori*[44]) are made from concentric layers of nanofibrils. According to these studies, the layers are nanofibrils in parallel arrangement, with an angle between the layers, leading to a "criss-crossing" pattern between nanofibrils in neighboring layers, which was reported for *Nephila*, *Latrodectus* and *B. mori* silk. Gould et al.[52] showed that as the strain in the fiber increases, this angle decreases. The authors suggested that as the fiber strand is extended, these nanofibrils are oriented toward the fiber axis.[52] However, since they only examined such patterns on the fiber surface, it is still unclear to what extent these changes also take place deeper within the fiber. After these three works, published 1996–2000, such interwoven patterns in silk were not further examined.

For the silk of the *Loxosceles* spider, in contrast, it has been shown that the nanofibrils run strictly parallel to the fiber axis.[12] Since the *Loxosceles* silk ribbon is only ≈ 50 nm thick, about 7 times thicker than an individual *Loxosceles* nanofibril, a layered organization of the fibrils in the ribbon is expected.

## Morphology and Structure of Nanofibrils

The observed fibril morphologies varied vastly across different works. Plated structures were reported by Li et al. (Fig. 2a),[25] while structures (slightly resembling fibrils) with round (Fig. 2b)[13] or elongated (Fig. 2e)[22] segments were observed on the surface and in the bulk of *Nephila* silk. In contrast, linear, featureless nanofibrils were observed in *Nephila* (Fig. 2d and f),[14,15,26,42] *Latrodectus* (Fig. 3-a and b),[52] *Loxosceles* (Fig. 4),[12] and *Nephilengys* (Fig. 3c and d)[17] silks.

To the best of our knowledge, the cross-sectional morphology of the nanofibrils has never been discussed. In most descriptions and models (see more details in the "Models of the Silk Structure" section below), the nanofibrils were simply assumed to have a circular cross-sectional profile. However, in our recent work with *Loxosceles* silk we found a noncircular cross section of the nanofibrils,[12] featuring a width of 20 nm and a thickness of 7 nm. This is not completely surprising since the cross section of this unusual silk fiber is highly asymmetric (6–8 $\mu$m in width, ≈ 50 nm in thickness, thus featuring an aspect ratio > 100:1), suggesting that the protein molecules are exposed to highly anisotropic local processing conditions during the spinning process. The recent work by Niu et al.[40] reported an exfoliation of *B. mori* silk nanofibrils into even smaller nano-ribbons that are 25 nm wide and 0.4 nm thick. This suggests a layered make-up of the nanofibrils, which would be compatible with nanofibrils of noncircular cross section. Recently, Parent et al.[62] examined the micellar structure in the spinning process using cryo-TEM and reconstruction of tomography tilt series, providing potential new research pathways for a better understanding of the natural silk nanofibril formation process.

## Mechanical Properties of Nanofibrils

The potentially significant role of nanofibrils in achieving the outstanding properties of silk has been discussed extensively.[12–24] Acquiring the mechanical properties of a single silk nanofibril and comparing it to the properties of the whole fiber seems to be a straightforward choice to further explore this issue. Theoretically, this can be achieved by an AFM probe picking up a single nanofibril and performing force spectroscopy (tensile testing). However, considering the extremely small dimension of nanofibrils, such experiments are challenging. Only a few studies reported such attempts: Oroudjev et al.[80] tested recombinant silk nanofibrils and Liu et al.[24] tested nanofibrils of *B. mori* silk. In both cases, the maximum force recorded was around 300 pN. Recent work from our group used another strategy: since nanofibrils are the only structural constituents in *Loxosceles* silk ribbons, the mechanical behavior exhibited by the whole ribbon has to be the sum of the

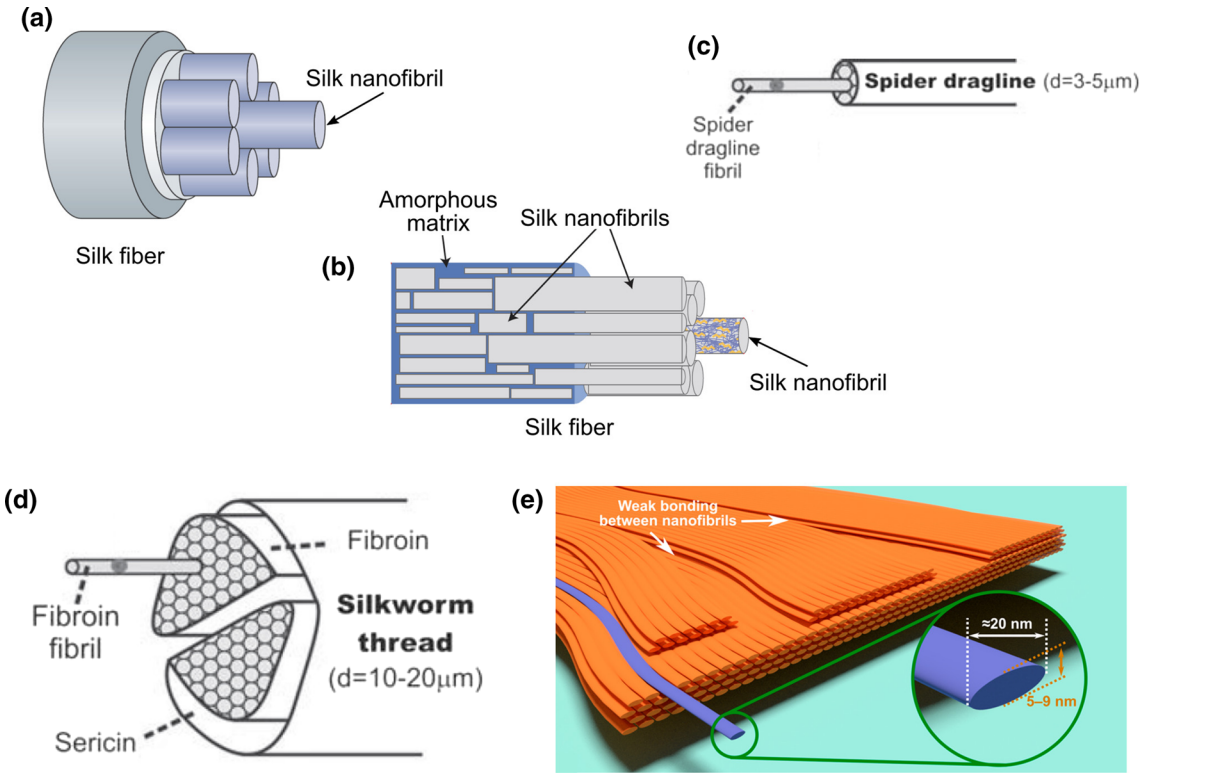


Fig. 7. Representative structural models for spider and silkworm silks. (a) Cylindrical spider MA silk featuring a skin–core organization.[19] (b) Variation of the model shown in (a). Nanofibrils of various lengths are embedded in amorphous matrix.[38] (c) Alternative model to describe the cylindrical spider MA silk,[23] where the whole silk fiber is composed of nanofibrils. (d) Structural model for *B. mori* silk featuring two bundles (brins) of fibroin wrapped by a layer of sericin.[23] (e) Structural model for *Loxosceles* ribbon silk.[12] Nanofibrils are arranged in a "pseudo-layered" fashion and loosely bonded. The nanofibrils in *Loxosceles* silk feature a noncircular shape. Permissions: (a) Adapted from Ref. 19. Copyright 2018 Springer Nature. (b) Adapted from Ref. 38. Copyright 2016 Springer Nature. (c, d) Adapted from Ref. 23. Copyright 2010 John Wiley and Sons. (e) Reprinted from Ref. 12. Copyright 2018 American Chemical Society.

mechanical contributions from the individual nanofibrils. Consequently, one can estimate the mechanical properties of an individual nanofibril by "down-scaling" a measured stress–strain curve of the whole ribbon to the cross section of an individual nanofibril. Following this approach, we estimated the breaking force of an individual nanofibril to be ≈ 120 nN,[12] which is 400 times more than previously reported.[24,80] This large discrepancy suggests that the previously estimated breaking forces were not large enough to explain the strength of silk. More experiments are needed with silks from different species to further elucidate this.

## MODELS OF THE SILK STRUCTURE

Over the past few decades, many models have been developed for the various hierarchical levels of spider and silkworm silk structures.[2,3,8,19,20,35] In Fig. 7, we show a selection representing most of the used structural models involving nanofibrils. Figure 7a[19] features one of the most frequently used models for cylindrical spider silk, depicted as a skin–core system, with silk nanofibrils occupying most of the core. Identical or slightly modified versions of this model were widely featured.[21,33–37,81] Given the significant experimental uncertainty with respect to some of the fundamental aspects of nanofibrils in silk fibers, we find it somewhat surprising, that these models were so widely adopted and promoted. While the skin–core organization has indeed been observed by several studies,[14,41,43] there is not a single piece of robust experimental evidence supporting a core "filled" with nanofibrils. As a matter of fact not a single experimental study presents any analysis or claim regarding the volume fraction of nanofibrils in silk. In other words, we do not know whether nanofibrils comprise 1% or 99% of a silk fiber. The skin layer in these models is usually drawn as a continuum, not featuring nanofibrils. This is also interesting, because experimental evidence showing nanofibrils is more easily obtained for the surface of a fiber than deeper inside the fiber.[13,17,52] Assuming that the core is indeed filled with nanofibrils, one can wonder how they are spatially organized and oriented. Most models simply draw straight, parallel fibrils, although several experiments have suggested twisted/angled organization[14,42,52] of the nanofibrils or a layered organization of the silk in general. In an evidence-based structural consensus model of silk, such details should be taken into account.

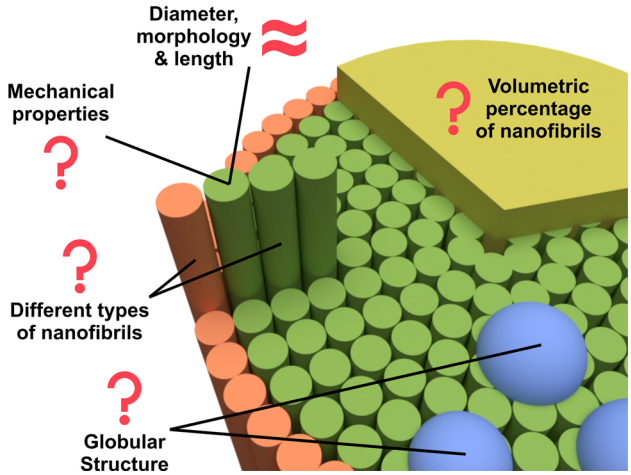


Fig. 8. Graphical summary representing some of the major unknowns about nanofibrils in silk fibers.

A variation of this model is featured in Fig. 7b, indicating nanofibrils of various diameters and lengths[38] embedded in an amorphous matrix. The idea of random nanofibril widths and lengths suggested by this particular model is not directly supported by evidence, as no consensus has been reached in regarding the diameter or length of nanofibrils in such fibers.

An alternative structural model for MA silk is shown in Fig. 7c,[23] where the silk fiber is entirely composed of fibrils rather than featuring a skin–core organization. In terms of experimental confirmation, this model suffers from the same issue mentioned above: the volumetric percentage is entirely unknown for cylindrical silks. Despite the significant uncertainty regarding the structure of silk fibers, several previous studies have suggested that the skin layer and core region have different mechanical behaviors[16,44] and carried out detailed simulations of mechanical properties based on such assumptions.[21,34,36,38] Structural models developed for silkworm silk are generally similar to the skin–core organization in spider silk, except that two bundles (brins) of fibroin are wrapped by the sericin coating (Fig. 7d).[23,40,43,47]

The *Loxosceles* ribbon silk is so far the only silk for which the structure at the nanofibril level has been completely revealed: it consists entirely of nanofibrils of a uniform, flattened cross section and thus does not feature a skin–core organization (Fig. 7e).[12] Its nanofibrils run strictly parallel to the fiber orientation and are organized in a "pseudo-layered" structure. We have further shown that the bonding strength between nanofibrils is small compared to the nanofibrils' tensile strength.[12]

## CONCLUSION

In summary, our review has shown that many studies have reported on nanofibrillar features in the natural silks of spiders and silkworms. However, due to experimental difficulties and due to the large number of silk producing species, the picture given by the evidence is incomplete (Fig. 8). The volumetric fraction of nanofibrils has not been established for any cylindrical silk. Limited information regarding nanofibril diameters is available; however, the proposed range is large, 3–300 nm. In several cases, contradicting data can be found, which may be due to differences in sample preparation, or due to particularities of the employed characterization techniques. Some studies have proposed a globular instead of nanofibrillar makeup of silk fibers altogether. To what degree silk fibers are skin–core structures has yet to be decided since different nanofibril diameters have been reported for different parts of the fiber. Similarly, limited information is available regarding the structural organization and distribution of nanofibrils within a silk fiber. Given how limited and sparse the reliable experimental evidence is, it is surprising how many detailed models and subsequent mechanical analyses on silk structures have been proposed and promoted. Future experimental work to resolve some of these ambiguities and open questions will greatly advance the silk field.

## ACKNOWLEDGEMENTS

This material is based upon work supported by the National Science Foundation under Grant No. DMR-1352542.

## REFERENCES

1. F. Vollrath and D.P. Knight, *Nature* 410, 541 (2001).
2. F.G. Omenetto and D.L. Kaplan, *Science* 329, 528 (2010).
3. J. Gosline, P. Guerette, C. Ortlepp, and K. Savage, *J. Exp. Biol.* 202, 3295 (1999).
4. I. Agnarsson, M. Kuntner, and T.A. Blackledge, *PLoS ONE* 5, e11234 (2010).
5. H.C. Schniepp, S.R. Koebley, and F. Vollrath, *Adv. Mater.* 25, 7028 (2013).
6. S.R. Koebley, F. Vollrath, and H.C. Schniepp, *Mater. Horiz.* 4, 377 (2017).
7. M. Andersson, Q. Jia, A. Abella, X.-Y. Lee, M. Landreh, P. Purhonen, H. Hebert, M. Tenje, C.V. Robinson, Q. Meng, G.R. Plaza, J. Johansson, and A. Rising, *Nat. Chem. Biol.* 13, 262 (2017).
8. M. Heim, D. Keerl, and T. Scheibel, *Angew. Chem. Int. Ed.* 48, 3584 (2009).
9. X.-X. Xia, Z.-G. Qian, C.S. Ki, Y.H. Park, D.L. Kaplan, and S.Y. Lee, *Proc. Natl. Acad. Sci.* 107, 14059 (2010).
10. A. Heidebrecht, L. Eisoldt, J. Diehl, A. Schmidt, M. Geffers, G. Lang, and T. Scheibel, *Adv. Mater.* 27, 2189 (2015).
11. A. Koeppel and C. Holland, *ACS Biomater. Sci. Eng.* 3, 226 (2017).
12. Q. Wang and H. C. Schniepp, *ACS Macro Lett.* 7, 1364 (2018).
13. N. Du, X.Y. Liu, J. Narayanan, L. Li, M.L.M. Lim, and D. Li, *Biophys. J.* 91, 4528 (2006).
14. A. Sponner, W. Vater, S. Monajembashi, E. Unger, F. Grosse, and K. Weisshart, *PLoS ONE* 2, e998 (2007).
15. M. Kitagawa and T. Kitayama, *J. Mater. Sci.* 32, 2005 (1997).
16. C. Riekel, M. Burghammer, T.G. Dane, C. Ferrero, and M. Rosenthal, *Biomacromol* 18, 231 (2017).
17. L.P. Silva and E.L. Rech, *Nat. Commun.* 4, (2013).
18. L.D. Miller, S. Putthanarat, R.K. Eby, and W.W. Adams, *Int. J. Biol. Macromol.* 24, 159 (1999).

19. S. Ling, D.L. Kaplan, and M.J. Buehler, *Nat. Rev. Mater.* 3, 18016 (2018).
20. M. Humenik, G. Lang, and T. Scheibel, *Wiley Interdiscip. Rev. Nanomed. Nanobiotechnol.* 10, e1509 (2018).
21. T. Giesa, M. Arslan, N.M. Pugno, and M.J. Buehler, *Nano Lett.* 11, 5038 (2011).
22. C.P. Brown, C. Harnagea, H.S. Gill, A.J. Price, E. Traversa, S. Licoccia, and F. Rosei, *ACS Nano* 6, 1961 (2012).
23. N. Du, Z. Yang, X.Y. Liu, Y. Li, and H.Y. Xu, *Adv. Funct. Mater.* 21, 772 (2010).
24. R. Liu, Q. Deng, Z. Yang, D. Yang, M.-Y. Han, and X.Y. Liu, *Adv. Funct. Mater.* 26, 5534 (2016).
25. S.F. Li, A.J. McGhie, and S.L. Tang, *Biophys. J.* 66, 1209 (1994).
26. D.P. Knight and F. Vollrath, *Philos. Trans. R. Soc. B Biol. Sci.* 357, 155 (2002).
27. S.E. Naleway, M.M. Porter, J. McKittrick, and M.A. Meyers, *Adv. Mater.* 27, 5455 (2015).
28. M.D. Shoulders and R.T. Raines, *Annu. Rev. Biochem.* 78, 929 (2009).
29. A.J.S. Fox, A. Bedi, and S.A. Rodeo, *Sports Health Multidiscip. Approach* 1, 461 (2009).
30. V. Ottani, D. Martini, M. Franchi, A. Ruggeri, and M. Raspanti, *Micron* 33, 587 (2002).
31. N. Mittal, F. Ansari, V.K. Gowda, C. Brouzet, P. Chen, P.T. Larsson, S.V. Roth, F. Lundell, L.W. Agberg, N.A. Kotov, and L.D. Söderberg, *ACS Nano* 12, 6378 (2018).
32. S. Ling, W. Chen, Y. Fan, K. Zheng, K. Jin, H. Yu, M.J. Buehler, and D.L. Kaplan, *Prog. Polym. Sci.* 85, 1 (2018).
33. W. Zhang, C. Ye, K. Zheng, J. Zhong, Y. Tang, Y. Fan, M.J. Buehler, S. Ling, and D.L. Kaplan, *ACS Nano* 12, 6968 (2018).
34. M.J. Buehler, *Nano Today* 5, 379 (2010).
35. L. Eisoldt, A. Smith, and T. Scheibel, *Mater. Today* 14, 80 (2011).
36. S. Keten, Z. Xu, B. Ihle, and M.J. Buehler, *Nat. Mater.* 9, 359 (2010).
37. I. Su and M.J. Buehler, *Nanotechnology* 27, 302001 (2016).
38. I. Su and M.J. Buehler, *Nat. Mater.* 15, 1054 (2016).
39. S. Ling, C. Li, K. Jin, D.L. Kaplan, and M.J. Buehler, *Adv. Mater.* 28, 7783 (2016).
40. Q. Niu, Q. Peng, L. Lu, S. Fan, H. Shao, H. Zhang, R. Wu, B.S. Hsiao, and Y. Zhang, *ACS Nano* 12, 11860 (2018).
41. K. Augsten, P. Mühlig, and C. Herrmann, *Scanning* 22, 12 (2000).
42. F. Vollrath, T. Holtet, H.C. Thogersen, and S. Frische, *Proc. R. Soc. B Biol. Sci.* 263, 147 (1996).
43. P. Poza, J. Pérez-Rigueiro, M. Elices, and J. Llorca, *Eng. Fract. Mech.* 69, 1035 (2002).
44. S. Putthanarat, N. Stribeck, S.A. Fossey, R.K. Eby, and W.W. Adams, *Polymer* 41, 7735 (2000).
45. M. Boulet-Audet, C. Holland, T. Gheysens, and F. Vollrath, *Biomacromolecules* 17, 3198 (2016).
46. J. Pérez-Rigueiro, M. Elices, G.R. Plaza, and G.V. Guinea, *Macromolecules* 40, 5360 (2007).
47. O. Hakimi, D.P. Knight, M.M. Knight, M.F. Grahn, and P. Vadgama, *Biomacromolecules* 7, 2901 (2006).
48. Y. Shen, M.A. Johnson, and D.C. Martin, *Macromolecules* 31, 8857 (1998).
49. D.C. Joy and J.B. Pawley, *Ultramicroscopy* 47, 80 (1992).
50. D.B. Williams and C.B. Carter, *Transmission Electron Microscopy* (New York: Springer, 1996), pp. 3–17.
51. Q. Wan, K.J. Abrams, R.C. Masters, A.C.S. Talari, I.U. Rehman, F. Claeyssens, C. Holland, and C. Rodenburg, *Adv. Mater.* 29, 1703510 (2017).
52. S.A.C. Gould, K.T. Tran, J.C. Spagna, A.M.F. Moore, and J.B. Shulman, *Int. J. Biol. Macromol.* 24, 151 (1999).
53. I. Greving, M. Cai, F. Vollrath, and H.C. Schniepp, *Biomacromolecules* 13, 676 (2012).
54. B.R. Neugirg, S.R. Koebley, H.C. Schniepp, and A. Fery, *Nanoscale* 8, 8414 (2016).
55. J. Pérez-Rigueiro, M. Elices, G.R. Plaza, J. Rueda, and G.V. Guinea, *J. Polym. Sci. Part B Polym. Phys.* 45, 786 (2007).
56. Z. Yang, D.T. Grubb, and L.W. Jelinski, *Macromolecules* 30, 8254 (1997).
57. D. Sapede, T. Seydel, V.T. Forsyth, M.M. Koza, R. Schweins, F. Vollrath, and C. Riekel, *Macromolecules* 38, 8447 (2005).
58. P.L. Babb, N.F. Lahens, S.M. Correa-Garhwal, D.N. Nicholson, E.J. Kim, J.B. Hogenesch, M. Kuntner, L. Higgins, C.Y. Hayashi, I. Agnarsson, and B.F. Voight, *Nat. Genet.* 49, 895 (2017).
59. E.R. Hoebeke, W. Huffmaster, and B.J. Freeman, *PeerJ* 3, e763 (2015).
60. D.P. Knight and F. Vollrath, *Philos. Trans. R. Soc. B Biol. Sci.* 357, 219 (2002).
61. A. Sponner, B. Schlott, F. Vollrath, E. Unger, F. Grosse, and K. Weisshart, *Biochemistry* 44, 4727 (2005).
62. L.R. Parent, D. Onofrei, D. Xu, D. Stengel, J.D. Roehling, J.B. Addison, C. Forman, S.A. Amin, B.R. Cherry, J.L. Yarger, N.C. Gianneschi, and G.P. Holland, *Proc. Natl. Acad. Sci.* 115, 11507 (2018).
63. R.W. Work, *Text. Res. J.* 47, 650 (1977).
64. G.P. Holland, J.E. Jenkins, M.S. Creager, R.V. Lewis, and J.L. Yarger, *Biomacromolecules* 9, 651 (2008).
65. P. Papadopoulos, R. Ene, I. Weidner, and F. Kremer, *Macromol. Rapid Commun.* 30, 851 (2009).
66. C.Y. Hayashi and R.V. Lewis, *BioEssays* 23, 750 (2001).
67. C.Y. Hayashi, *Mol. Biol. Evol.* 21, 1950 (2004).
68. E. Gnesa, Y. Hsia, J.L. Yarger, W. Weber, J. Lin-Cereghino, G. Lin-Cereghino, S. Tang, K. Agari, and C. Vierra, *Biomacromolecules* 13, 304 (2012).
69. A. Rising, G. Hjälm, W. Engström, and J. Johansson, *Biomacromolecules* 7, 3120 (2006).
70. G.V. Guinea, M. Elices, G.R. Plaza, G.B. Perea, R. Daza, C. Riekel, F. Agulló-Rueda, C. Hayashi, Y. Zhao, and J. Pérez-Rigueiro, *Biomacromolecules* 13, 2087 (2012).
71. W. Eberhard and F. Pereira, *J. Arachnol.* 21, 161 (1993).
72. G. Xu, L. Gong, Z. Yang, and X.Y. Liu, *Soft Matter* 10, 2116 (2014).
73. L.-S. Dai, C. Qian, L. Wang, G.-Q. Wei, Q.-N. Liu, Y. Sun, C.-F. Zhang, J. Li, D.-R. Liu, B.-J. Zhu, and C.-L. Liu, *J. Asia-Pac. Entomology* 18, 701 (2015).
74. A. Bram, C.I. Brändén, C. Craig, I. Snigireva, and C. Riekel, *J. Appl. Crystallogr.* 30, 390 (1997).
75. C. Riekel, M. Rössle, D. Sapede, and F. Vollrath, *Naturwissenschaften* 91, 30 (2004).
76. C. Riekel and F. Vollrath, *Int. J. Biol. Macromol.* 29, 203 (2001).
77. C. Riekel, B. Madsen, D. Knight, and F. Vollrath, *Biomacromolecules* 1, 622 (2000).
78. C. Riekel, C. Bränden, C. Craig, C. Ferrero, F. Heidelbach, and M. Müller, *Int. J. Biol. Macromol.* 24, 179 (1999).
79. D.T. Grubb and L.W. Jelinski, *Macromolecules* 30, 2860 (1997).
80. E. Oroudjev, J. Soares, S. Arcidiacono, J.B. Thompson, S.A. Fossey, and H.G. Hansma, *Proc. Natl. Acad. Sci.* 99, 6460 (2002).
81. A. Tarakanova and M.J. Buehler, *JOM* 64, 214 (2012).